Correlation between Molecular Packing and Surface Potential at Vanadyl Phthalocyanine/HOPG Interface

ARTICLE *in* THE JOURNAL OF PHYSICAL CHEMISTRY C · OCTOBER 2010

Impact Factor: 4.77 · DOI: 10.1021/jp1076565

4 AUTHORS, INCLUDING:

Weiguang Xie
Jinan University (Guangzhou, China)
55 PUBLICATIONS **346** CITATIONS
SEE PROFILE

Kun Xue
The Chinese University of Hong Kong
29 PUBLICATIONS **247** CITATIONS
SEE PROFILE

Correlation between Molecular Packing and Surface Potential at Vanadyl Phthalocyanine/HOPG Interface

Weiguang Xie, Jianbin Xu,* Jin An, and Kun Xue

Department of Electronic Engineering and Materials Science and Technology Research Center, The Chinese University of Hong Kong, Shatin, Hong Kong

Received: August 13, 2010; Revised Manuscript Received: October 4, 2010

We report on the thickness-dependent morphology and surface potential of vanadyl phthalocyanine (VOPc) ultrathin films due to the variations between lying-down and tilted molecular packing configurations at the interface of VOPc film/highly ordered pyrolytic graphite (HOPG). Transition from a bilayer-thickness-dependent distribution to an orientation-dependent inhomogeneity of surface potential is observed in the same film. The surface potential change in the initial lying-down bilayers can be described by the abrupt junction model. In areas thicker than ca. 6 nm, a potential energy difference of about 100 meV between differently oriented VOPc molecular layers is found, indicating that the boundaries act as significant barriers for hole transport.

Correlation between the organic molecular packing structures such as staking, steric orientation, domain size, and grain boundary with the energy level alignment at the interface is of scientific and technological interest due to its close association in understanding the interfacial carrier accumulation and transfer in organic electronic/photonic devices. Thickness-dependent interfacial properties can be revealed by light-induced emission or absorption techniques.[1−6] However, the spatial resolution of these techniques hardly reaches submicrometer scales;[7] therefore the correlation between nanostructures and electronic properties at the interface is less known. Fortunately, a highly spatially resolved image of interfacial structure and surface potential can be achieved by scanning Kelvin probe microscopy (SKPM) and related techniques, as has been demonstrated at the interface of pentacene/SiO_2 by Frisbie et al.[8,9]

Metallophthalocyanine (MPc) is one type of promising molecular material for organic devices due to its superior device performance, stability, and low cost. Although the thickness and temperature dependent molecular orientation,[10−13] vacuum energy level alignment,[1,2] and the orientation-induced charge transfer[3−5] of planar MPc molecules, e.g., CuPc and F_{16}CuPc, have been intensively studied by photoelectron emission spectroscopy (PES),[6] near-edge X-ray absorption fine structure (NEXAFS) measurement,[2,10] metastable-atom electron spectroscopy (MAES),[4] and scanning probe microscopy[10,11] on different substrates,[14,15] nonplanar MPc's, e.g., TiOPc and VOPc, are relatively unexplored at interfaces on a nanoscopic scale. Especially, nonplanar MPc based organic devices were found to have better device performance.[16−18]

In this work, we investigate the correlation between surface potential and VOPc molecular stacking at the interface of VOPc/HOPG by exploiting SKPM and ultrahigh vacuum scanning tunneling microscopy (UHV-STM). Highly ordered pyrolytic graphite (HOPG) surface is chosen in this case, as its surface is atomic flat and electrically conductive, which may be resemble to the metal/organic interface in organic devices. In addition, the contact angle of HOPG is 75°,[19] just between the commonly used gate dielectrics of SiO_2 (18°)[16,20] and OTS/SiO_2 (104°)[16] in organic transistors. The HOPG surface is also commonly used substrate for optical spectroscopic techniques, thus the nanoscopic studies are easily comparable to the macroscopic ones.

* Author to whom correspondence should be addressed, jbxu@ee.cuhk.edu.hk.

Results and Discussion

The growth of VOPc ultrathin film on a HOPG surface has been interrogated by in situ UHV-STM and ex situ atomic force microscopy (AFM) at room temperature. Figure 1 shows the growth of VOPc molecules on HOPG observed by STM. When the VOPc film is thin in Figure 1a, the VOPc molecules form islands on the HOPG surface. The height of each island is about 0.74 nm, similar to the thickness of one bilayer. This observation is consistent with the former studies showing that the VOPc molecules arrange in a cofacial configuration to cancel their own dipoles.[21,22] A HOPG surface can still be observed in Figure 1a, indicating the bilayer islands do not fully cover the surface. No island thicker than one bilayer is observed. When the film grows thicker, we find that the islands would first grow to form a fully covered bilayer. Only when the first fully covered bilayer is formed can nanoislands with thickness of one or more bilayers be grown on the first bilayer. The observed growth of VOPc molecules on HOPG can be described by the Stranski−Krastanov growth model that the fully covered first layer acts as a buffer layer to reduce the effect of lattices mismatch between VOPc thin film and HOPG so that thicker islands can grow. A lattice resolved STM image of the VOPc bilayer is showed in Figure 1c. The base lattice vectors are $a = 12.98$ Å and $b = 13.94$ Å, and the angle is $\theta = 89.9°$. The difference between a and b should be due to the existence of thermal drift at room temperature.

Figure 2 shows the SKPM measurement on VOPc ultrathin film near the freshly cleaved HOPG surface. Because of the HOPG surface corrugations on a submicrometer scale, it is not easy to distinguish VOPc thin film from HOPG surface via the topography image. However, in the phase image, the HOPG surface on the left indeed shows a darker contrast than VOPc molecules on the right. Although the phases of the first bilayer and the higher order bilayers are almost the same, higher order bilayers can be distinguished from their respective morphological variations and heights as indicated in Figure 2e.

10.1021/jp1076565
Published on Web 10/20/2010

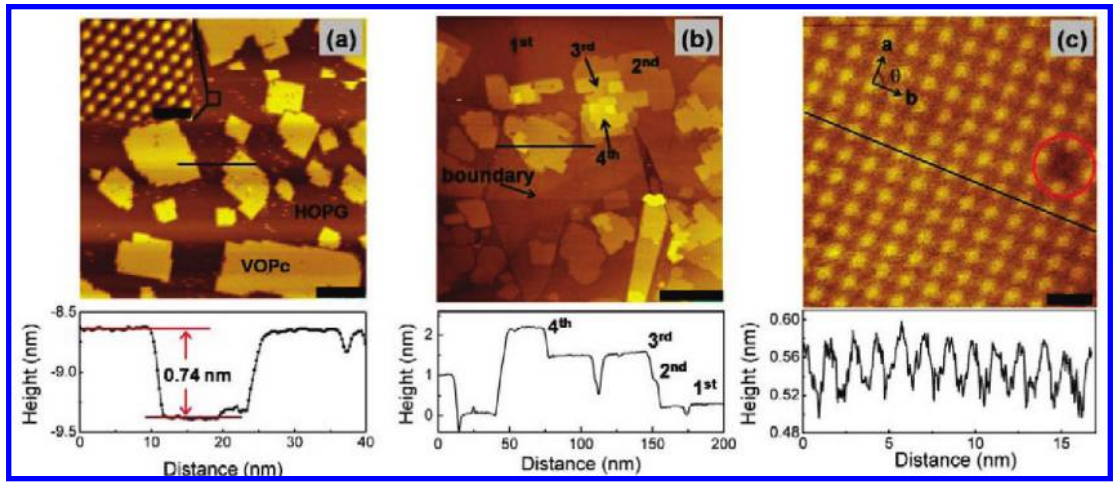

Figure 1. STM image of (a) 0.28 nm VOPc molecules on HOPG surface. The scale bar is 20 nm. The inset shows the atomic surface of HOPG substrate. The scale bar is 0.5 nm. (b) More than one bilayer of VOPc molecules on HOPG. The scale bar is 100 nm. (c) High-resolution image of VOPc molecules on the surface. The circle indicates a defect site due to a missing molecule. The scale bar is 2 nm. The curves at the lower parts of (a), (b), and (c) are the line profiles along the black lines in the images separately. The imaging condition is ~1.5 V, ~20−40 pA.

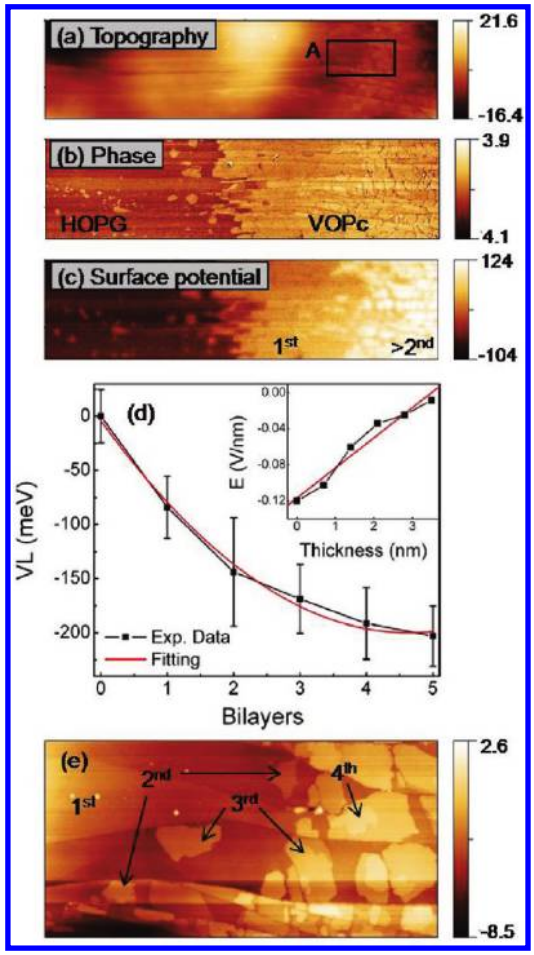

Figure 2. (a−c) Surface topographic, phase images and surface potential distribution at the VOPc/HOPG edge (10 × 2.5 μm^2). (d) Bilayer-dependent vacuum level (VL) of VOPc at the interface (the vacuum level of HOPG is the reference). Note that the bright contrast in the surface potential distribution here indicates higher surface potential but lower vacuum level. (e) Zoom-in topographic image of the rectangle area *A* in (a) (2.5 × 1.5 μm^2). Units for the color bars of topographic, phase images and surface potential distribution are nanometers, degrees, and millielectronvolts, respectively.

At the same time, the associated surface potential distribution shows that the surface potential alterations are strongly correlated to the bilayers at the interface. The bilayer-dependent

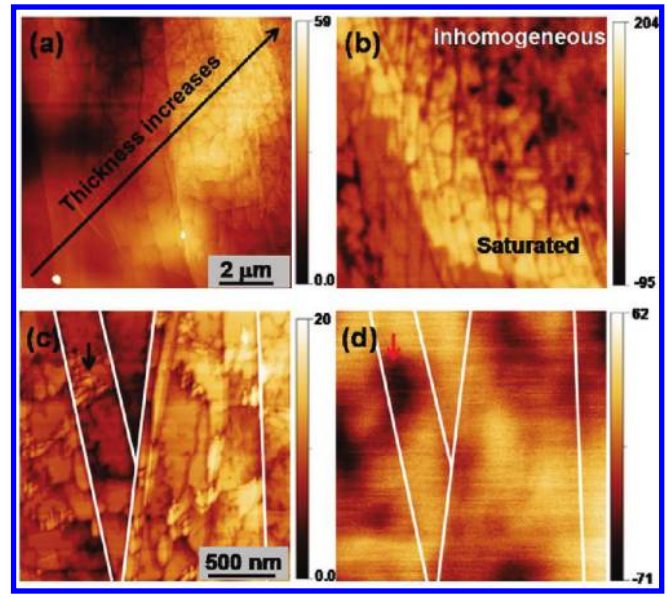

Figure 3. (a, c) Surface topographic images of VOPc ultrathin film on HOPG. The unit for the color bar is nanometers. (b, d) Associated surface potential distributions of (a) and (c), respectively. Unit for the color bar is millivolts. The white lines are added for comparison.

vacuum level change in Figure 2d is calculated from the surface potential values of the regions with different number of bilayers. We can see that the vacuum level of the VOPc ultrathin film decreases as the film thickness (or the number of bilayers) increases, indicating existence of dipoles at the interface. We also find that the surface potential is saturated after the ultrathin film extends to 5−7 bilayers (ca. 3.5−4.9 nm), where the vacuum level of different bilayers against that of HOPG tends to remain a constant value of about 200 meV (Figure 3b). In the vicinity of the interfacial bilayers, we find that the bilayer-dependent vacuum level can be well-described by the commonly used abrupt junction model for inorganic semiconductor interface. By solving the Poisson equation over the interfacial bilayers, the vacuum level can be written as

$$V = V_0 + (\rho/2\varepsilon_r\varepsilon_0)(x - x_0)^2 \quad (0 < x < x_0) \qquad (1)$$

where V_0 is a constant related to the reference energy, ρ is the areal charge density, and x_0 is the width of the transition region.

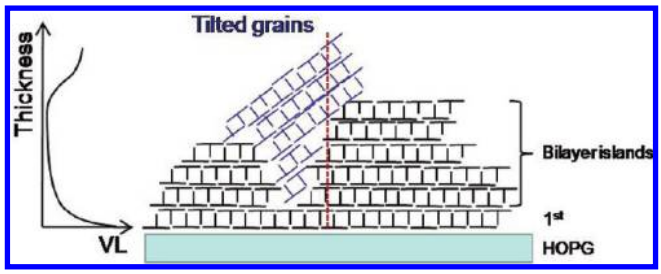

Figure 4. The potential-energy diagram in the left schematically shows the vacuum level variation along the red dash line in the molecular packing. For drawing convenience, the tilt of molecules is exaggerated, and only the cofacial features of the two phases are shown.

Figure 2d shows the fitting of the experimental data by using eq 1. The inset shows the linear relation of the built-in electrical field with the thickness and the slope equal to $\rho/\varepsilon_r\varepsilon_0$.

Around the thicker areas (about >6 nm), different morphological patterns, as well as large fluctuations of surface potential, can be observed. A typical example is showed in panels a and b of Figure 3, where the film at the upper-right side is thicker than that in the lower left. Figure 3b shows that the thicker upper-right area has the relatively smaller surface potential than the saturated area. Moreover, the distribution is inhomogeneous at the nanometer scale. From the topographic image, it can be seen that the surface is composed of not only flat islands but also numerous grains. An enlarged area is showed in panels c and d of Figure 3, indicating the morphological attributes and the corresponding surface potential distribution. For example, the grains, as indicated by the black arrow in Figure 3c, aggregate with the adjacent flat islands. The surface potential is generally lower in the areas where the grains aggregate. Study on the initial growth of VOPc molecules by our STM measurement shows that grains tend to be initiated at the HOPG step edges or VOPc nanoscale-island boundaries. The grains observed by STM have tilted planes with tilted angles varying from 0° to 5.79° with respect to the surface of vicinal lying down bilayers, and the diameter of the grains can be more than 100 nm. Grains with larger tilted angles should exist in the thick areas that cannot be imaged using STM. Occurrence of tilted grains is also confirmed by XRD characterization. It is seen that only the epitaxial growth is dominant when the film is ultrathin, while VOPc molecules with bulk α-phase molecular packing coexist after the film grows thicker. Therefore, we determine that the grains are composed of the tilted molecules.

Although the steric orientation and thickness dependent energy alignment variations of metallophthalocyanine at interface have been reported from UPS/PES experiments,[1−4] the local characteristics are rarely explored. The nanoscopic scenario that correlates the interfacial molecular packing with the vacuum level of VOPc/HOPG is schematically shown in Figure 4. The vacuum level shifting ΔU_{VL} can be given as[22]

$$\Delta U_{VL} = \Delta U_{dip} + \Delta U_{tr} \qquad (2)$$

where ΔU_{dip} is the shifting due to the polarized dipole in the molecule and ΔU_{tr} is the shifting due to the charge transfer. Although the VOPc molecule is a polar molecule, the intrinsic dipole in the bilayer is canceled due to the opposite dipole direction of the upper and lower molecules. The vacuum level shift due to the inductive dipole and charge transfer in vacuum is also small (<10 meV).[22,23] However, in ambient conditions, the situation is very different. As defects such as boundaries, island steps, and vacancy (as showed in panels b and c of Figure 1) exist in the film, oxygen molecules in the atmosphere are able to diffuse into the defects and couple with the adjacent molecules via a charge transfer process

$$\mathrm{VOPc} + \mathrm{O_2} \rightleftharpoons \mathrm{VOPc} + \mathrm{O_2^{-\delta}} + \delta\mathrm{h^+} \qquad (3)$$

The doping effect to VOPc can be supported from the mobility measurement from a VOPc based FET device. A VOPc thin film shows p-type behavior with hole mobility of 0.3−1.0 $cm^2\ V^{-1}\ s^{-1}$ in the atmosphere, while the hole mobility decreases to about 1.4×10^{-4} $cm^2\ V^{-1}\ s^{-1}$ at 10^{-2}−10^{-3} Pa. Moreover, bipolar behavior is observed in vacuum.[16] The ΔU_{tr} term thus change greatly due to the doping effect. Assuming that the relative dielectric constant of lying-down VOPc is 1.22 as that of TiOPc,[22] we can determine that the interfacial charge transfer between oxygen-doped VOPc and HOPG is 2.1×10^{-3}e/molecule (1.4×1.4 nm^2) from the slope of a built-in electrical field.

The significant vacuum level shift at interface induces a strong built-in maximum electrical field of ~0.12 V/nm between the HOPG and the first bilayers (Figure 2d). Also we can estimate from the literature that the built-in electrical field (E_{bin}) at some interface is in the order of magnitude of 0.1−1 V/nm.[24−26] Such a built-in electrical field should not be ignored in myriads of interfacial processes. For example, considering a simple Coulomb model, the interacting electrical field between hole−electron pair is $E_{int} = e/4\pi\varepsilon_0\varepsilon_r r^2 = 1.44/\varepsilon_r r_0^2$ V/nm, where ε_r is the relative dielectric constant of molecule and r_0 is the distance of the electron and hole in nanometers. As r_0 in organic molecules equals to or is bigger than the size of one molecule in many cases, E_{int} should fall in the region of the observed E_{bin}. The built-in electrical field thus affects the diffusion and injection of electron/hole at organic/metal as well as the separation/recombination of electron−hole pair.[27] Note that such an obvious band-bending type attribute at the interface may be not expected in polymers and a few small molecules under UHV conditions, because the charge density in the molecules is less and the charges are localized. However, such a behavior has been demonstrated by UPS in π-conjugated organic thin films.[28,29]

The existence of tilted metallophthalocyanine molecules when the film grows thick is observed by light-induced absorption or emission techniques.[30−32] The reason for the tilted of molecules is considered to be due to the weakening of substrate−molecule interaction. Here we observed that tilted grains are only nucleated locally adjacent to the boundaries of lying-down islands or on the HOPG steps at the initial growth. Different molecule stacking behavior at steps is also reported with F_{16}CuPc adsorbed on Cu(111) using STM.[33] The observation in nanoscale suggests that the surface morphology plays a key role in the completion between intramolecule interaction and molecule−substrate interaction and may determine the tilted angle of molecules. As the dielectric constants of MPc's are highly anisotropy,[34] the tilted molecules would lead to a dramatic change in inductive ΔU_{dip}, thus leading to the change in vacuum level shift. Inhomogeneous distribution of the vacuum level is observed in the thicker areas of the VOPc thin film where the density and size of the tilted grains increase to a critical value. The observed maximum energy difference in the vicinity of the boundaries among sterically orientated molecules (tilted and lying down) is about 100 meV. This energy is much higher than the thermal energy at room temperature (ca. 26 meV). Therefore, the boundaries of sterically orientated molecules should act as an effectual blocking barrier for hole transport.

In summary, the nanoscopic scenario on the correlation between interfacial morphology and surface potential distribution is revealed at the interface of VOPc/HOPG. We find that VOPc molecules are initially arranged in lying-down configuration on a HOPG surface, and the surface potential variation is described by the abrupt junction model. The nucleation of tilted grains at the boundaries is observed in thicker areas, which results in inhomogeneous surface potential in the film.

Experimental Section

VOPc molecules are purchased from Alfa Aesar and purified by three cycles of sublimation. HOPG is cleaved in air and then immediately transferred into the deposition chamber with a base vacuum of 2×10^{-8} mbar. VOPc molecules are deposited onto HOPG at a rate of 0.5−1.0 nm/min. During the deposition, the HOPGs are kept at room temperature. STM characterization is performed in a RHK UHV 300 STM system with base pressure of 1×10^{-9} mbar. Surface potential measurement is taken by employing a Nanoscope IIIa in air. Before the measurement, one part of the HOPG surface is cleaved as a reference for surface potential characterization. X-ray diffraction (XRD) patterns are acquired with a Bruker D5005 X-ray diffactometer.

Acknowledgment. We thank Mr. J. Du and Mr. X. Wan for their technical support and stimulating discussion. This work is in part supported by the Research Grants Council of Hong Kong, particularly, via Grant Nos. CUHK2/CRF/08 and CUHK4182/09E. J. B. Xu thanks the National Science Foundation of China for the support, particularly, via Grant Nos. 60990314 and 60928009.

References and Notes

(1) Tang, J. X.; Lee, C. S.; Lee, S. T. Electronic structures of organic/organic heterojunctions: from vacuum level alignment to Fermi level pinning. *J. Appl. Phys.* **2007**, *101*, 064504-1−064504-4.

(2) Toader, T.; Gavrila, G.; Ivanco, J.; Braun, W.; Zahn, D. R. T. Controlling geometric and electronic properties of highly ordered CuPc thin films. *Appl. Surf. Sci.* **2009**, *255*, 6806–6808.

(3) Chen, W.; Chen, S.; Chen, S.; Huang, Y. L.; Huang, H.; Qi, D. C.; Gao, X. Y.; Ma, J.; Wee, A. T. S. Orientation-controlled charge transfer at CuPc/F_{16}CuPc interfaces. *J. Appl. Phys.* **2009**, *106*, 064910-1−064910-4.

(4) Yamane, H.; Yabuuchi, Y.; Fukagawa, H.; Kera, S.; Okudaira, K. K.; Ueno, N. Does the molecular orientation induce an electric dipole in Cu-phthalocyanine thin films. *J. Appl. Phys.* **2006**, *99*, 093705-1−093705-5.

(5) Chen, W.; Huang, H.; Chen, S.; Huang, Y. L.; Gao, X. Y.; Wee, A. T. S. Molecular orientation-dependent ionization potential of organic thin films. *Chem. Mater.* **2008**, *20*, 7017–7021.

(6) Xiao, J.; Dowben, P. A. The role of the interface in the electronic structure of adsorbed metal(II) (Co, Ni, Cu) phthalocyanines. *J. Mater. Chem* **2009**, *19*, 2172–2178.

(7) Sugiyama, T.; Sasaki, T.; Kera, S.; Ueno, N.; Munakata, T. Photoemission microspectroscopy and imaging of bilayers islands formed in monolayer titanyl phthalocyanine films. *Chem. Phys. Lett.* **2007**, *449*, 319–322.

(8) Kalihari, V.; Ellison, D. J.; Haugstad, G.; Frisbie, C. D. Observation of unusual homoepitaxy in ultrathin pentacene films and correlation with surface electrostatic potential. *Adv. Mater.* **2009**, *21*, 3092–3098.

(9) Puntambekar, K.; Dong, J.; Haugstad, G.; Frisbie, C. D. Structural and electrostatic complexity at a pentacene/insulator interface. *Adv. Funct. Mater.* **2006**, *16*, 879–884.

(10) Huang, Y. L.; Chen, W.; Chen, S.; Wee, A. T. S. Low-temperature scanning tunneling microscopy and near-edge X-ray absorption fine structure investigation of epitaxial growth of F_{16}CuPc thin films on graphite. *Appl. Phys. A: Mater. Sci. Process.* **2009**, *95*, 107–111.

(11) Takada, M.; Tada, H. Low temperature scanning tunneling microscopy of phthalocyanine multilayers on Au(111) surfaces. *Chem. Phys. Lett.* **2004**, *392*, 265–269.

(12) Kataoka, T.; Fukagawa, H.; Hosoumi, S.; Nebashi, K.; Sakamoto, K.; Ueno, N. Observation of temperature-dependent transition of a copper-phthalocyanine thin film adsorbed on HOPG. *Chem. Phys. Lett.* **2008**, *451*, 43–47.

(13) Doherty, W. J.; Friedlein, R.; Salaneck, W. R. Layer-by-layer deposition of copper phthalocyanine from aqueous solution: molecular orientation ordering parameters and electronic structure. *J. Phys. Chem. C* **2007**, *111*, 2724–2729.

(14) Wang, S. D.; Dong, X.; Lee, C. S.; Lee, S. T. Orderly growth of copper phthalocyanine on hightly oriented pyrolytic graphite (HOPG) at high substrate temperatures. *J. Phys. Chem. B* **2004**, *108*, 1529–1532.

(15) Chen, W.; Huang, H.; Chen, S.; Gao, X. Y.; Wee, A. T. S. Low-temperature scanning tunneling microscopy and near-edge x-ray absorption fine structure investigations of molecular orientation of copper(II) phthalocyanine thin films at organic heterojunction interfaces. *J. Phys. Chem. C* **2008**, *112*, 5036–5042.

(16) Li, L. Q.; Tang, Q. X.; Li, H. X.; Hu, W. P. Molecular orientation and interface compatibility for high performance organic thin film transistor based on vanadyl phthalocyanine. *J. Phys. Chem. B* **2008**, *112*, 10405–10410.

(17) Wang, H. B.; Song, D.; Yang, J. L.; Yu, B.; Geng, Y. H. Yan D. H.; High mobility vanadyl-phthalocyanine polycrystalline films for organic field-effect transistors. *Appl. Phys. Lett.* **2007**, *90*, 253410-1–253410-3.

(18) Li, L. Q.; Tang, Q. X.; Li, H. X.; Yang, X. D.; Hu, W. P.; Song, Y. B.; Shuai, Z. G.; Xu, W.; Liu, Y. Q.; Zhu, D. B. An ultra closely p-stacked organic semiconductor for high performance field-effect transistors. *Adv. Mater.* **2007**, *19*, 2613–2617.

(19) Wang, R.; Sakai, N.; Fujishima, A.; Watanabe, T.; Hashimoto, K. Studies of surface wettability conversion on TiO_2 single-crystal surface. *J. Phys. Chem. B* **1999**, *103*, 2188–2194.

(20) Yu, X. J.; Xu, J. B.; Cheung, W. Y.; Ke, N. Optimizing the growth of vanadyl-phthalocyanine thin films for high-mobility organic thin-film transistors. *J. Appl. Phys.* **2007**, *102*, 103711-1–103711-6.

(21) Yanagi, H.; Mikami, T.; Tada, H.; Terui, T.; Mashiko, S. Molecular stacking in epitaxial crystals of oxometal phthalocyanines. *J. Appl. Phys.* **1997**, *81*, 7306–7312.

(22) Fukagawa, H.; Yamane, H.; Kera, S.; Okudaira, K. K.; Ueno, N. Experimental estimation of the electric dipole moment and polarizability of titanyl phthalocyanine using ultraviolet photoelectron spectroscopy. *Phys. Rev. B* **2006**, *73*, 041302-1−041302-4.

(23) Fukagawa, H.; Yamane, H.; Kera, S.; Okudaira, K. K.; Ueno, N. UPS fine structures of highest occupied band in vanadyl-phthalocyanine ultrathin film. *J. Electron Spectrosc. Relat. Phenom.* **2005**, *144*, 457–477.

(24) Molodtsova, O. V.; Knupfer, M. Electronic properties of the organic semiconductor interfaces CuPc/C_{60} and C_{60}/CuPc. *J. Appl. Phys.* **2006**, *99*, 053704-1−053704-7.

(25) Brumbach, M.; Placencia, D.; Armstrong, N. R. Titanyl phthalocyanine/C_{60} heterojunctions: Band-edge offset and photovoltaic device performance. *J. Phys. Chem. C* **2008**, *112*, 3142–3151.

(26) Gassenbauer, Y.; Klein, A. Electronic and chemical properties of tin-doped surfaces and ITO/ZnPc interfaces studied in-situ by photoelectron spectroscopy. *J. Phys. Chem. B* **2006**, *110*, 4793–4801.

(27) Gulbinas, V.; Zaushitsyn, Y.; Sundström, V.; Hertel, D.; Bässler, H.; Yartsev, A. Dynamics of the electric field-assisted charge carrier photogeneration in ladder-type poly(para-phenylene) at a low excitation intensity. *Phys. Rev. Lett.* **2002**, *89*, 107401-1–107401-4.

(28) Nishi, T.; Kanai, K.; Ouchi, Y.; Willis, M. R.; Seki, K. Evidence for the atmospheric p-type doping of titanyl phthalocyanine thin film by oxygen observed as the change of interfacial electronic structure. *Chem. Phys. Lett.* **2005**, *414*, 479–482.

(29) Ishii, H.; Hayashi, N.; Ito, E.; Washizu, Y.; Sugi, K.; Kimura, Y.; Niwano, M.; Ouchi, Y.; Seki, K. Kelvin probe study of band bending at organic semiconductor/metal interfaces: examination of Fermi level alignment. *Phys. Status Solidi A* **2004**, *201*, 1075–1094.

(30) Wang, L.; Qi, D. C.; Liu, L,; Chen, S.; Gao, X. Y.; Wee, A. T. S. Molecular orientation and ordering during initial growth of copper phthalocyanine on Si(111). *J. Phys. Chem. C* **2007**, *111*, 3454–3458.

(31) Peisert, H.; Biswas, I.; Zhang, L.; Knupfer, M.; Hanack, M.; Dini, D.; Cook, M. J.; Chambrier, I.; Schmidt, T.; Batchelor, D.; Chassé, T. Orientation of substituted phthalocyanines on polycrystalline gold: distinguishing between the first layers and thin films. *Chem. Phys. Lett.* **2005**, *403*, 1–6.

(32) Okudaira, K. K.; Hasegawa, S.; Ishii, H.; Seki, K.; Harada, Y.; Ueno, N. Structure of copper-and H_2-phthalocyanine thin films on MoS_2 studied by angle-resolved ultraviolet photoelectron spectroscopy and low energy electron diffraction. *J. Appl. Phys.* **1999**, *85*, 6453–6461.

(33) Wakayama, Y. Assembly process and epitaxy of the F_{16}CuPc monolayer on Cu(111). *J. Phys. Chem. C* **2007**, *11*, 2675–2678.

(34) Ramprasad, R.; Shi, N. Polarizability of phthalocyanine based molecular systems: A first-principles electronic structure study. *Appl. Phys. Lett.* **2006**, *88*, 222903-1–222903-3.

JP1076565